

Nanowire-Based Nanoelectronic Devices in the Life Sciences

Fernando Patolsky, Brian P. Timko, Gengfeng Zheng, and Charles M. Lieber

Abstract

The interface between nanosystems and biosystems is emerging as one of the broadest and most dynamic areas of science and technology, bringing together biology, chemistry, physics, biotechnology, medicine, and many areas of engineering. The combination of these diverse areas of research promises to yield revolutionary advances in healthcare, medicine, and the life sciences through the creation of new and powerful tools that enable direct, sensitive, and rapid analysis of biological and chemical species. Devices based on nanowires have emerged as one of the most powerful and general platforms for ultrasensitive, direct electrical detection of biological and chemical species and for building functional interfaces to biological systems, including neurons. Here, we discuss representative examples of nanowire nanosensors for ultrasensitive detection of proteins and individual virus particles as well as recording, stimulation, and inhibition of neuronal signals in nanowire–neuron hybrid structures.

Introduction

Semiconductor nanowires are emerging as remarkably powerful building blocks in nanoscience, with the potential to have a significant impact on numerous areas of science and technology ranging from electronics and photonics to the life sciences and healthcare.^{1–9} Critical to the advances now being made worldwide with nanowires has been the well-developed understanding of the growth mechanism,^{1–6,10} which has enabled the reproducible synthesis of nanowires of homogeneous composition and diameter with controllable electronic and optical properties. Moreover, predictable elaboration of the basic nanowire structural motif has been utilized to produce axial heterostructures and superlattices, radial core–shell and core–multishell heterostructures, and branched nanowire structures with unique functions built in at the stage of synthesis.^{2–6} Significantly, these characteristics make semiconductor nanowires one of the best defined and most versatile

nanomaterial systems available today, thus enabling scientists to move beyond, for example, single-device proof-of-concepts studies to the exploration of new areas of science and technology.

One particularly rich area centers on the interface between nanowires and the life sciences. In general, the similarity in size of nanowires and natural nanostructures in biological systems makes nanowires an obvious choice for creating highly sensitive tools that can probe biological systems. Nanowire electronic devices, moreover, enable a detection and sensing modality—direct and label-free electrical readout (i.e., without the use of bound dyes or fluorescent probes)—that is exceptionally attractive for many applications in medicine and the life sciences.^{7–9,11–15} Here, we provide an introduction to the underlying nanowire nanotechnology and then illustrate the diverse applications of this technology at the interface with the biological sciences.

Nanowire Field-Effect Sensors

Underlying detection using semiconductor nanowires is their configuration as field-effect transistors (FETs), which exhibit a conductivity change in response to variations in the electric field or potential at the surface of the device.^{11,16–19} In a standard FET, the conductance of the semiconductor between the source and drain is modulated between on and off states by a third gate electrode capacitively coupled through a thin dielectric layer to the semiconductor.²⁰ In the case of a *p*-type semiconductor, applying a negative gate voltage leads to an accumulation of majority charge carriers (positive holes) and a corresponding increase in conductance. The dependence of the conductance on gate voltage and corresponding charge at the gate electrode/dielectric interface makes FETs natural candidates for electrically based sensing, since the binding of a charged or polar biological or chemical species to the gate dielectric is analogous to applying a voltage using a gate electrode. For example, binding of a protein with net negative charge to the surface of a *p*-type FET will lead to an accumulation of positive hole carriers and an increase in device conductance.

Nanowires composed of silicon or other semiconductors can also function as FET devices.^{2,3,16–19} Critical to overcoming the sensitivity limitations of planar FET sensors is the one-dimensional morphology of nanowires. An analyte binding to the surface of a nanowire can lead to depletion or accumulation of carriers through the entire cross section of the device, versus only a thin region near the surface of a planar device;¹¹ that is, the binding event will lead to a much greater change in device conductance for the nanowire versus a planar FET.

Nanowire-based sensing devices can be configured from high-performance FETs by linking specific receptor groups to the surface of the nanowire.^{7–9,11–15} When these surface-modified devices are exposed to a solution containing a macromolecule species such as a protein, specific binding to the receptor will lead to an increase or decrease in the device conductance depending on the net charge of the biomolecule and the semiconductor type (*p* or *n*), as illustrated in Figure 1a. An important point about this detection process, which is quite distinct from common optically based assays, is that it occurs in real time, and the binding process can be viewed as it happens on a computer logging the conductance of one or more devices.

To explore this very broad and widely applicable concept, we have developed an

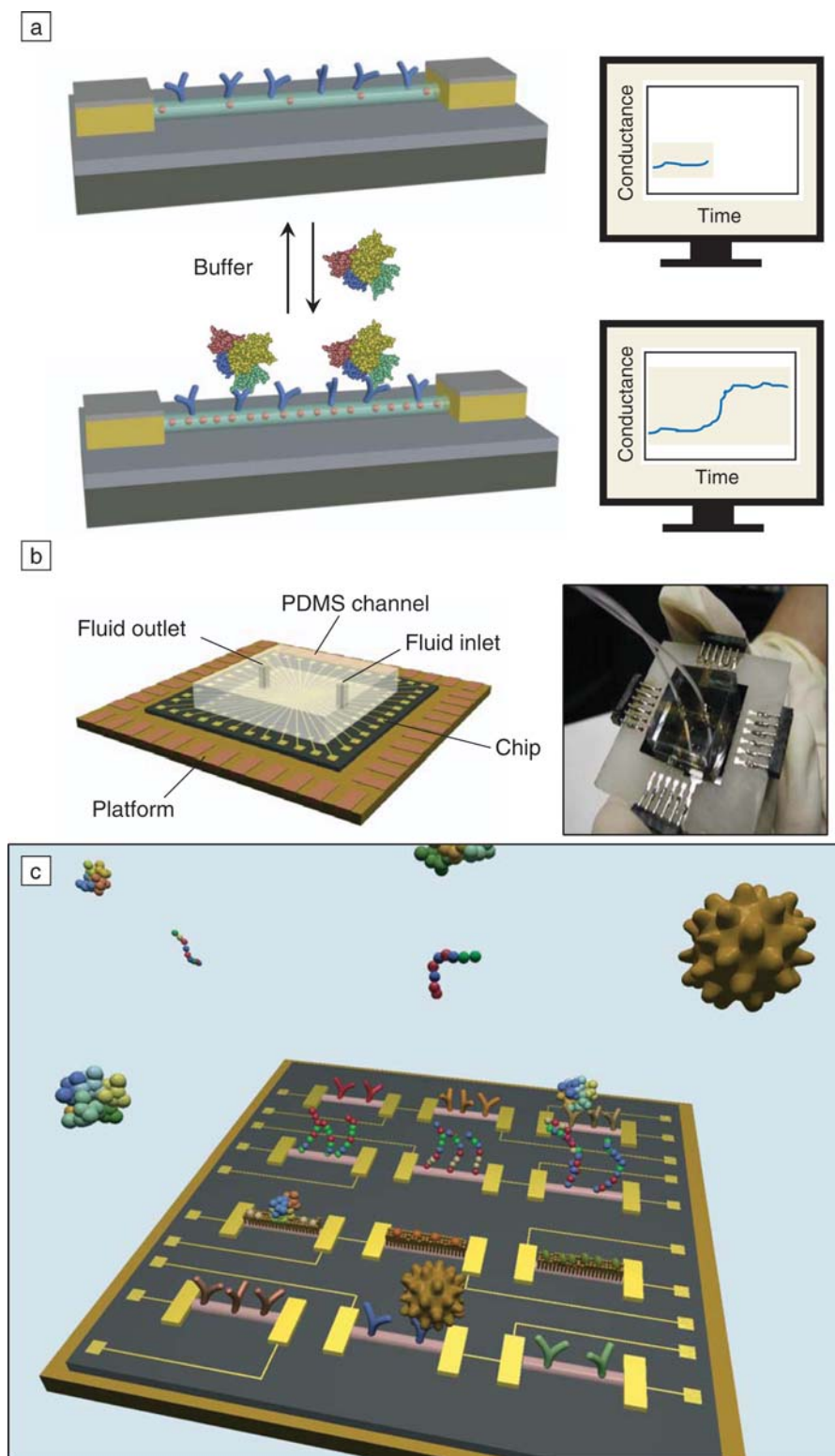


Figure 1. (a), (left) Schematic illustration of a nanowire field-effect transistor configured as a sensor with antibody receptors (blue). (right) Binding of a protein with a net negative charge to a *p*-type nanowire yields an increase in conductance. (b), (left) Schematic and (right) photograph of a prototype nanowire sensor biochip with integrated microfluidic sample delivery. (c) Schematic of a nanowire device array for multiplexed, real-time sensing of multiple biological species. The size of the chip is about $15\ \mu\text{m} \times 15\ \mu\text{m}$.

integrated microfluidic/nanowire sensing platform that incorporates nanowires with well-defined *p*- and/or *n*-type dopants, specifically tailored surface functionality, source and drain electrodes that are insulated from the fluid environment by a dielectric passivation layer, and a polymer-embedded microfluidic channel that enables rapid solution delivery to arrays of nanowire devices, as shown in Figure 1b.^{7-9,14,15} In addition, the small size of the nanowire devices not only enables very high-sensitivity detection, as discussed earlier, but also allows for tens to hundreds of individually addressable nanowire devices to be defined within a single microfluidic delivery channel. Significantly, defining distinct surface receptors on different nanowire elements opens up the potential for multiplexed, real-time assays of multi-component solutions, such as the simultaneous detection of proteins, DNA, viruses, and small molecules, as shown in Figure 1c. This general platform therefore provides a route toward screening of complex biological fluids and could thereby have a broad impact on the life sciences.

Multiplexed, Real-Time, Label-Free Detection of Proteins

The first example of electrical detection of proteins in solution using nanostructures was reported by our group using single *p*-type silicon nanowire devices in 2001.¹¹ More recently, we developed the use of nanowire devices for the detection of multiple disease marker proteins simultaneously in a single versatile detection platform.¹⁵ Electrically addressable arrays are fabricated by a process that uses fluid-based assembly of nanowires to align and set the average spacing of nanowires over large areas,²¹ and then photolithography and metal deposition to define interconnects to a large number of individual nanowires in parallel, as shown in Figure 2a. The active area of a state-of-the-art nanowire sensor array fabricated in this way and containing more than 100 independently addressable nanowire elements is shown in Figure 2b, where the addressable elements are in columns (marked with a blue rectangle), repeating across the center of the image, that overlap with a microfluidic channel mated to the chip for operation.

Device arrays prepared in this way offer unique opportunities for label-free multiplexed detection of biological species such as disease marker proteins. An important result of ongoing genomics and proteomics research is the elucidation of many new biomarkers that have potential for greatly improving the diagnosis of diseases.²² The availability of multiple biomarkers is

believed to be especially important in the diagnosis of complex diseases like cancer,²³ where disease heterogeneity makes single-marker tests, such as the analysis of prostate-specific antigen (PSA), inadequate.

The development of silicon nanowire sensor arrays for cancer biomarker detection has been carried out by attaching monoclonal antibodies to the nanowire elements following device fabrication.^{13,15} Sensitivity limits for cancer marker protein detection using this new generation of silicon nanowire device arrays were determined by measuring conductance changes as the solution concentration of PSA was varied, where the devices were modified with monoclonal antibodies for PSA (PSA-Ab1). A *p*-type silicon nanowire device (NW1 in Figure 2c) showed a well-defined conductance increase and subsequent return to baseline when PSA solution (points 1 and 2) and pure buffer (indicated by arrows), respectively, were alternately delivered through the microfluidic channel to the devices. Notably, these data show that direct, label-free detection of PSA is routinely achieved with a signal-to-noise ratio of >3 for concentrations down to 75 fg/ml, or approximately 2 fM.¹⁵

The reproducibility and selectivity of the nanowire devices was further demonstrated in competitive binding experiments (Figure 2c, points 3 and 4), which showed no conductance changes following delivery of concentrated bovine serum albumin (BSA) or PSA-Ab1 (PSA pre-blocked by reacting with a specific antibody, Ab1) solutions. In addition, a second control nanowire element, a *p*-type silicon nanowire device passivated with ethanolamine, was monitored in parallel (Figure 2c, NW2). Significantly, simultaneous measurements of the conductance of NW1 and NW2 show that well-defined concentration-dependent conductance increases are only observed in NW1 upon delivery of PSA solutions, with no response observed for NW2. This simple implementation of multiplexing represents a highly robust means for discriminating against false positive signals arising from either electronic noise or non-specific binding and represents a powerful advantage of this nanotechnology.¹⁵

The unique multiplexing capabilities of nanowire device arrays have been exploited in other significant ways. First, distinct *p*- and *n*-type nanowire device elements have been incorporated in single sensor chips, and data recorded simultaneously from a *p*-type nanowire (Figure 2d, NW1) and an *n*-type nanowire (Figure 2d, NW2) showed a reversible conductance increase and decrease, respectively, during delivery of

PSA followed by buffer solutions (indicated by the arrows). These complementary electrical signals provide a simple yet robust means for detecting false positive signals

from either electrical noise or nonspecific binding of protein; that is, real and selective binding events must show complementary responses in the *p*- and *n*-type devices.

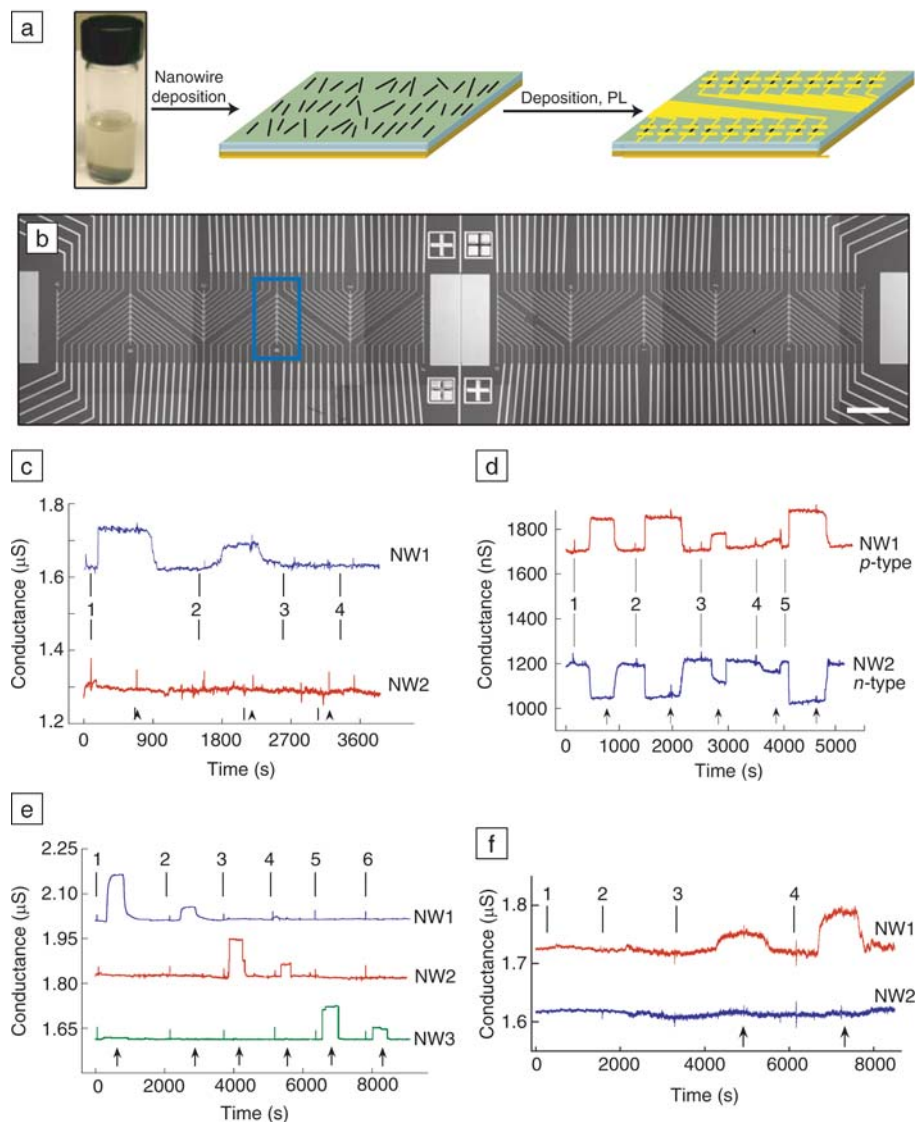


Figure 2. (a) Overview of the steps in fabricating nanowire arrays for a sensor chip. Nanowires suspended in ethanol in a vial are deposited onto a substrate wafer. Photolithography followed by metallization defines contacts to the nanowires. (b) Optical image of a portion of a nanowire array; the blue rectangle indicates one column of individually addressable elements. Scale bar is 300 μm. (c) Data recorded simultaneously from two p-Si nanowire devices, where NW1 was functionalized with prostate-specific antigen (PSA-Ab1), and NW2 was modified with ethanolamine. Points 1–4 correspond to times when solutions of (1) 9 pg/ml PSA, (2) 1 pg/ml PSA, (3) 10 μm/ml bovine serum albumin (BSA), and (4) 1 ng/ml PSA + 10 μm/ml PSA-Ab1 were added. Arrows correspond to the points where the solution was switched to buffer. (d) Complementary sensing of PSA using p-type (NW1) and n-type (NW2) nanowire devices. Points 1–5 correspond to the addition of PSA solutions of (1, 2) 0.9 ng/ml, (3) 9 pg/ml, (4) 0.9 pg/ml, and (5) 5 ng/ml. (e) Simultaneous detection of PSA, carcinoembryonic antigen (CEA), and mucin-1 using NW1, NW2, and NW3 functionalized with antibodies for PSA, CEA, and mucin-1, respectively. Protein solutions of (1, 2) PSA, (3, 4) CEA, and (5, 6) mucin-1 were delivered sequentially to the array. (f) Conductance versus time data recorded for the detection of PSA in donkey serum samples with (1) buffer, (2) serum, and (3, 4) serum and PSA. NW2 was passivated with ethanolamine. (Adapted from Reference 15.)

More generally, multiplexed detection of distinct disease marker proteins, which will facilitate pattern analysis of existing and emerging markers for robust diagnosis, can be carried out with high sensitivity and selectivity using nanowire arrays modified with distinct antibody receptors, as shown in Figure 2e. This critical capability was demonstrated in reported studies of PSA (a prostate cancer biomarker), carcinoembryonic antigen (CEA, a colon cancer biomarker), and mucin-1 (a breast cancer biomarker) detection using silicon nanowire devices functionalized with monoclonal antibody receptors for PSA (NW1), CEA (NW2), and mucin-1 (NW3).¹⁵ Conductance measurements recorded simultaneously from NW1, NW2, and NW3 as different protein solutions were sequentially delivered to the device array (Figure 2e) demonstrated clearly multiplexed real-time, label-free marker protein detection with sensitivity to the femtomolar level and essentially 100% selectivity.

Ultimately, rapid cancer diagnosis for healthcare will require rapid analysis of clinically relevant samples such as blood serum. A unique feature of our nanotechnology is that analysis of one or many markers can be achieved from literally a drop of blood, in contrast to standard serum analysis today requiring milliliters of blood and extensive laboratory work-up. We demonstrated this key advance using the nanowire arrays to detect PSA in undiluted serum samples.¹⁵

Notably, conductance versus time data recorded simultaneously from NW1, which was modified with a PSA-Ab1 receptor, and NW2, which was passivated with ethanolamine, show that serum containing 59 mg/ml total protein did not lead to an appreciable conductance change relative to the standard assay buffer, while serum containing PSA led to concentration-dependent conductance increases only for NW1 (Figure 2f). Well-defined conductance changes were observed for PSA concentrations as low as 0.9 pg/ml, which corresponds to a concentration ~100 billion times lower than that of the background serum proteins.

These results demonstrate unambiguously that nanowire sensor arrays can be used to detect multiple cancer markers rapidly with high sensitivity and selectivity in undiluted human serum in samples as small as one drop of blood. Given that our studies have demonstrated the basic principles underlying nanowire sensor arrays for ultrasensitive detection, we believe that commercialization will lead to an exciting and powerful technology for advancing human healthcare.

Detection of Single Viruses

The studies just reviewed implicitly show exquisite sensitivity unmatched by any other existing label-free sensor device, yet they do not define the ultimate sensitivity of the nanowire FET devices. To address this critical issue and explore the broad-based application of nanowire devices for biosensing, our group carried out studies of the detection of viruses,¹⁴ which are among the most important causes of human disease and an increasing concern as agents for biological warfare and terrorism, with the goal of determining whether the ultimate limit of one single virus could be reliably detected.

The concept underlying our experiments is as follows (Figure 3a, left): When a single virus particle binds to a receptor linked to the surface of a nanowire FET detector, it yields a conductance change due to the change in surface charge; when the virus particle subsequently unbinds, the conductance returns to baseline.¹⁴ Significantly, delivery of highly dilute influenza A virus solutions, on the order of 80 attomolar (10^{-18} M) or 50 viruses/ μ L, to *p*-type silicon nanowire devices modified with monoclonal antibodies for influenza A produced well-defined, discrete conductance changes (Figure 3a, red curve) that are characteristic of binding and unbinding of single positively charged influenza viruses.¹⁴ Definitive proof that the discrete conductance changes observed in these studies were due to binding and unbinding of a single virus was obtained from simultaneous optical and electrical measurements using fluorescently labeled influenza viruses. The optical and electrical data in Figure 3a (right) show that as a virus diffuses near a nanowire device, the conductance remains at the baseline value, and only after binding at the nanowire surface does the conductance drop in a quantized manner similar to that observed with unlabeled viruses. As the virus unbinds and diffuses from the nanowire surface, the conductance returns rapidly to the baseline value. These parallel measurements also show that a virus must be in contact with the nanowire device to yield an electrical response, thus suggesting that it will be possible to develop ultradense nanowire device arrays without crosstalk from nearby but not specifically bound viruses, with the minimum size scale simply set by that of the virus.

Selective detection, the ability to specifically distinguish one type of virus from another, is crucial for exploiting the high sensitivity of these nanowire devices in most medical and bio-threat applications. We have demonstrated clear selectivity in multiplexing experiments that could en-

able powerful advances, for example, in rapid medical diagnosis. Specifically, *p*-type silicon nanowire sensor elements in an array (Figure 3b, top) were modified with monoclonal antibody receptors specific for influenza A (NW1) and adenovirus (NW3), and in addition, a control nanowire element (NW2), which was passivated with ethanolamine, was included. Simultaneous conductance measurements obtained when adenovirus, influenza A, and a mixture of both viruses were delivered to the device array (Figure 3b, bottom) demonstrate several significant points. First, delivery of adenovirus, which is negatively charged at the pH of the experiment,¹⁴ to the device array yields positive conductance changes for NW3 with an on time similar to the selective binding/unbinding in single-device experiments. Well-defined binding/unbinding events are not observed from the nanowire device modified with the influenza virus receptor. Second, delivery of influenza A solutions yields negative conductance changes for NW1 similar to the single-device measurements of Figure 3a, while well-defined binding/unbinding is not observed on NW3. In both cases, no evidence of binding/unbinding was found in the control element, NW2. Last, delivery of a mixture of both viruses demonstrates unambiguously that selective binding/unbinding responses for adenovirus and influenza A can be detected in parallel by NW3 and NW1, respectively, at the single-virus level. Significantly, the simplicity, single viral particle sensitivity, and selective multiplexed detection capability demonstrate unambiguously that nanowire sensors could serve as the key element in powerful viral sensing devices for medical and bioterrorism applications in the future.

Nanowire/Neuron Artificial Synapses

Electrophysiological measurements made using micropipette electrodes and microfabricated electrode arrays have and continue to play an important role in understanding the electrical behavior of individual neurons and neuronal networks.^{24,25} Micropipette electrodes can stimulate and record intracellular and extracellular potentials *in vitro* and *in vivo* with relatively good spatial resolution,^{24,26} yet are difficult to multiplex. Microfabricated structures, such as electrode and FET arrays, have potential for large-scale multiplexing, and have enabled recording from both individual neurons and neural networks.^{25,27–32} However, these microfabricated structures have not been sufficiently small or sensitive to detect and stimulate neuronal

activity at the level of individual axons and/or dendrites.

To address these issues, which could include complementary studies of signal propagation and inhibition important to neural processing, and also to explore the potentially rich interface between nanoelectronic and biological systems, we have recently reported the assembly and electrical characterization of hybrid structures consisting of nanowire FET arrays and patterned neurons.³³ Individual nanowire devices are attractive for interfacing with neurons because the contact length along an axon or dendrite projection crossing a nanowire is only on the order of 20 nm; that is, they are highly local and noninvasive probes of neuronal projections.

Our strategy for preparing nanowire/neuron devices (Figure 4a) involves assembly of oriented *p*- and/or *n*-type silicon nanowires,^{15–19} interconnection into FET device array structures,^{7–9,15,34} patterning of an adhesion and growth factor to define neuron cell growth with respect to the device elements, and neuron growth under standard conditions.³³ This overall approach is flexible, allowing for (1) variations in the

array geometry and addressable nanowire device separations, (2) incorporation of electronically distinct *p*- and *n*-type elements in well-defined positions, and (3) variation in the number and spatial location of the hybrid nanowire/neuron junctions with respect to the cell body and neurite projections.

An optical image of an array consisting of a repeating 1-neuron/1-nanowire motif with the soma (cell body) spatially remote and the axon (long and narrow projection) directed across the respective nanowire element (Figure 4b, left and center) shows a high yield of 1:1 hybrid live cell/nanowire devices with selective growth of the axon verified by marker-specific fluorescence labeling and multicolor confocal microscopy (Figure 4b, far right).³³ Notably, the typical active junction area for devices, about 0.01–0.02 μm^2 , is orders of magnitude smaller than microfabricated electrodes and planar FETs. The small hybrid junction sizes (about 20 nm wide), which are similar to natural synapses, offer important advantages compared to other electrophysiological methods; these advantages include spatially resolved detection of signals

without complications of averaging extracellular potential changes over a large percentage of a given neuron, and integration of multiple elements on the axon and dendrite projections from a single neuron.

We assessed electrical communication in the neuron–nanowire structures by eliciting action potential spikes using a conventional glass microelectrode while simultaneously recording the intracellular potential and conductance at the microelectrode and nanowire FET, respectively.³³ Figure 4c shows the direct temporal correlation between the potential spikes initiated and recorded in the soma and the corresponding conductance peaks measured by the nanowire at the axon–nanowire junction. The direct correlation of the nanowire conductance peaks with intracellular potential peaks is expected for *p*-type nanowires used for this experiment, since the relative potential at the outer membrane becomes more negative and then more positive (opposite to the measured intracellular potential), causing an accumulation of carriers/enhanced conductance and depletion/reduced conductance, respectively.²⁰ A number of distinct control experiments

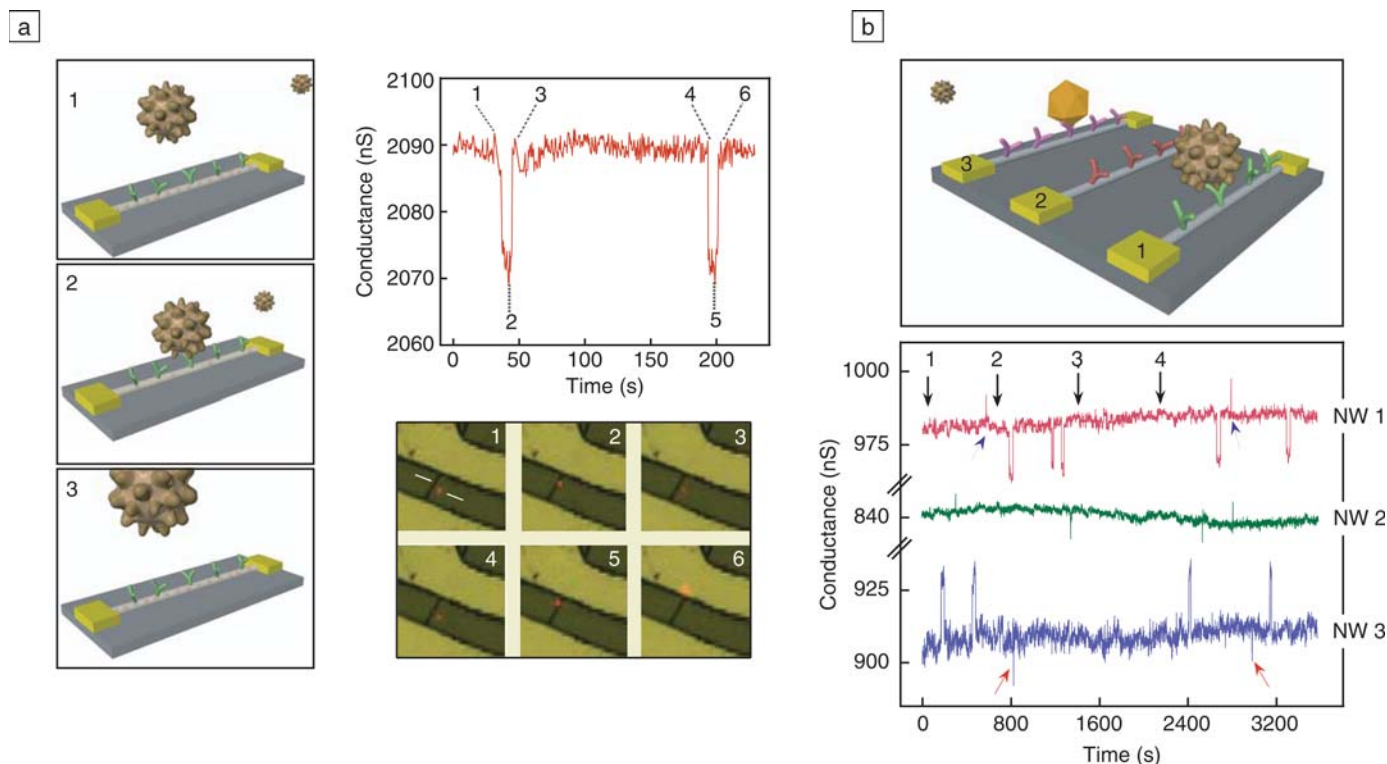


Figure 3. (a), (left, 1–3) Schematic illustration of a single virus binding and unbinding to the surface of a silicon nanowire device modified with antibody receptors. (right, top) Simultaneous conductance versus time data and (right, bottom) optical images recorded from a single nanowire device modified with anti-influenza type A antibody. (b), (top) Schematic of multiplexed single-virus detection. (bottom) Conductance versus time data recorded simultaneously from three nanowire elements, where NW1 was modified with antibody for influenza A (red curve), NW2 was modified with ethanolamine only (green curve), and NW3 was modified with antibody for adenovirus (blue curve). Arrows 1–4 correspond to the introduction of adenovirus, influenza A, pure buffer, and a 1:1 mixture of adenovirus and influenza A, respectively. (Adapted from Reference 14.)

demonstrate clearly that the nanowire conductance spikes correspond to direct and localized detection of the action potential propagating along the neuronal axons.³⁴ Nanowire devices were also used to stimulate neuronal activity through nanowire/axon junctions. Application of biphasic excitatory pulse sequences to the nanowire of nanowire/axon junctions (Figure 4d) results in somatic action potential spikes, which are detected with the intracellular electrode. The excitation shows a threshold of about 0.4 V, where no potential spikes were observed with the intracellular electrode when driving the nanowire below this threshold value. Significantly, we have also shown that a single nanowire can be used for simultaneous stimulation and detection of potential spikes.³⁴

We further exploited the flexibility of our approach though the assembly and characterization of hybrid nanowire/neuron devices in which the number and spatial arrangement of nanowires interfaced to the axons and dendrites were varied.³³ For example, a device structure consisting of a linear array of four-nanowire FETs, a gap, and five-nanowire FETs was designed to investigate simultaneous and temporally resolved forward propagation and backward propagation of action potential spikes in axons and dendrites, respectively. An optical image (Figure 5a) demonstrates well-defined growth of cortical neurons, with the cell body localized in the gap between the nanowires and an axon and dendrite guided by chemical patterning in opposite directions across the two linear nanowire FET arrays.³⁴

Significantly, we showed that stimulation of action potential spikes in the soma yields correlated conductance peaks in nanowire elements forming the nanowire/axon and nanowire/dendrite junctions, as seen in Figure 5b.³³ Qualitatively, these data demonstrate several key points and highlight the unique power of merging nanowire-based nanoelectronics with neuroscience. First, seven of the nine independently addressable nanowire/neurite junctions yield reproducible conductance spikes correlated with intracellular stimulation. While previous studies using glass microelectrodes have recorded spike propagation in axons and dendrites,^{35,36} axon/dendrite propagation has not been measured simultaneously nor has the same level or recording points been achieved; furthermore, microfabricated FETs and electrodes have never measured propagation in single cells previously. Second, these noninvasive studies and data have allowed quantitative analysis of the propagation rate and mechanism of neuronal signals. Specifically, the conductance spikes recorded along the axon by elements 1–5 maintain a sharp peak shape and relatively constant peak amplitude (Figure 5c, right), and the conductance spikes measured by elements 6–9 along the dendrite exhibit noticeable broadening and reduced amplitude (Figure 5c, left). These peak-shape variations are consistent with known mechanisms of active (peak shape is maintained) and passive (peak decays over distance) transport in axons and dendrites, respectively.^{33,37} Furthermore, the temporal separation between the spatially separated nanowire elements yields propagation rates of 0.16 m/s and 0.43 m/s for dendrites and axons, respectively.

Our unique nanoscale approach, which is distinct from previous work with microfabricated planar FETs and microelectrodes,^{24–32} has also been extended to highly integrated systems that open up opportunities in a number of areas.³³ For example, we designed and fabricated a structure consisting of 50 addressable nanowire elements per neuron, as shown in Figure 5d, an unprecedented level of integration for nanoelectronic–biological systems. An optical image (Figure 5d) shows that well-aligned neuron growth over dense nanowire device arrays is routinely possible. Moreover, electrical transport measurements demonstrated that intracellular stimulation of action potentials in the soma yield a mapping of the spike propagation by the 50 devices over the approximately 500- μ m-long axon (Figure 5e). Beyond this demonstration of electrical interfacing, which exploits the unique control and reproducibility of nanowire devices, we have also used nanowire/neuron

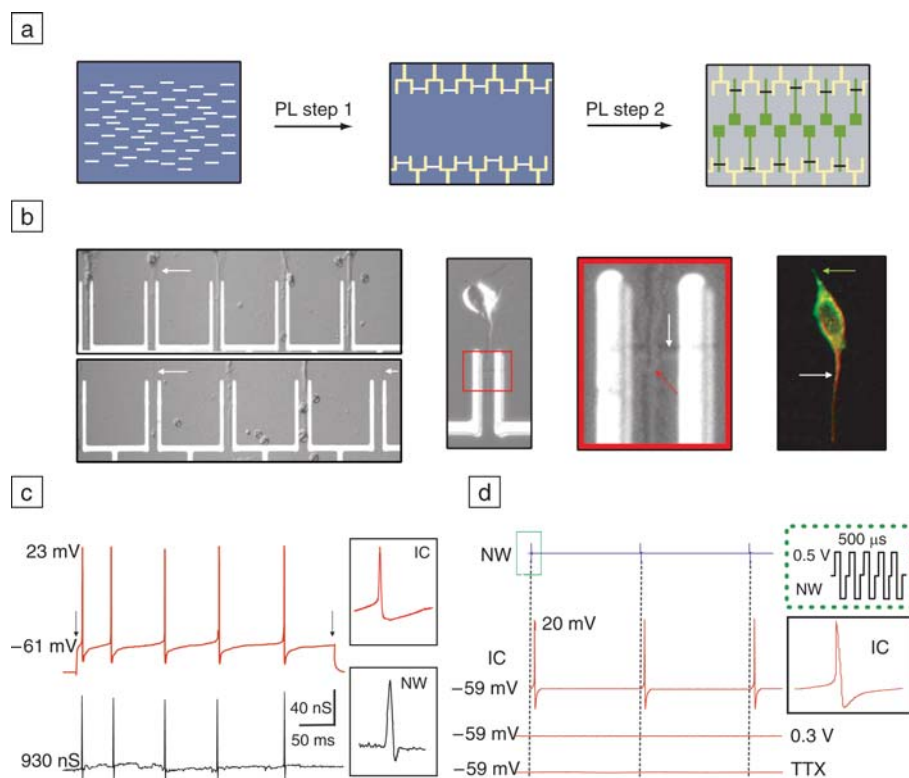


Figure 4. (a) Overview of the preparation of aligned neuron/nanodevice array. First, nanowires are aligned on a substrate chip. Two subsequent photolithography (PL) steps are used to define metallic contacts and chemical functionalization, respectively. (b), (left and center) Optical images of directed growth of cortical neurons on a silicon nanowire array. (far right) Confocal fluorescence image of a dual-color-labeled cortex neuron after 4 days in culture, highlighting the axon (red area indicated by white arrow) and short dendrite (green area indicated by green arrow). Spacing between source/drain electrodes is 5 μ m. (c) Intracellular (IC) potential (red) and silicon nanowire conductance (black) following IC stimulation. Nanowire conductance is plotted in nanosiemens (nS). (d) Local axon–nanowire stimulation (black dotted lines) and correlated IC electrical recording (red traces) of a rat cortex neuron. The upper-right inset is an expansion (from the left) of the nanowire stimulation sequence. IC plots recorded stimuli of (upper red trace) 0.5 V amplitude, (middle red trace) 0.3 V amplitude, and (lower red trace) 0.5 V amplitude after bath application of 0.5 μ M tetrodotoxin (TTX). (Adapted from Reference 33.)

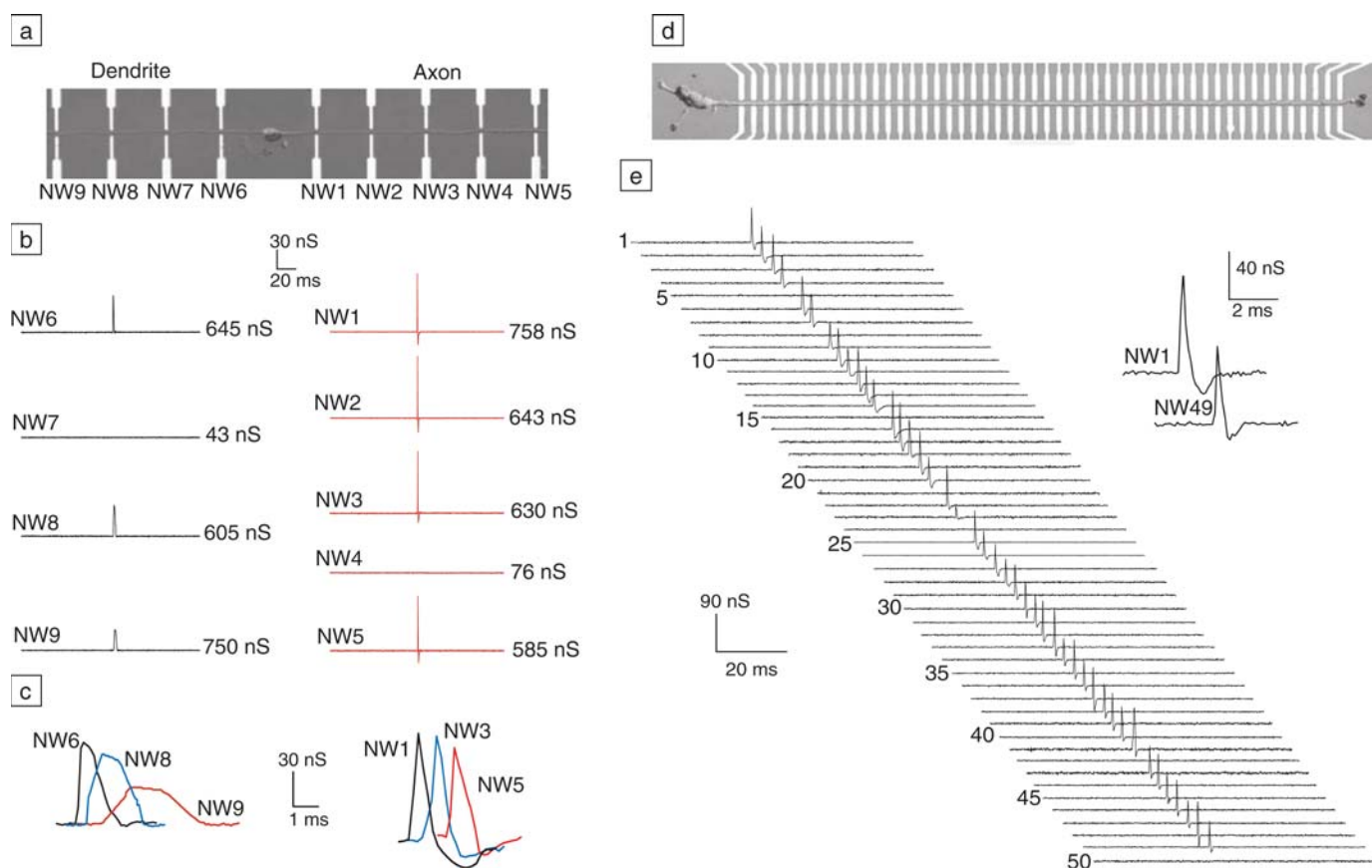


Figure 5. (a) Optical image of a cortex neuron with axon and dendrite aligned in opposite directions. Inter-electrode spacing is 50 μm . (b) Electrical responses measured from dendrite/nanowire devices (left, NW6–NW9) and axon/nanowire devices (right, NW1–NW5) after intracellular stimulation. No responses were measured from NW4 and NW7 due to poor nanowire/metal contacts. (c) Expansion of peaks from (b), elucidating the evolution of peak shape as it propagates along each process. (d) Optical image of aligned axon crossing an array of 50 devices. Inter-electrode spacing is 10 μm . (e) Electrical data from the 50-device array shown in (d). (Adapted from Reference 33.)

structures to demonstrate novel hybrid electronic devices, including the demonstration of complementary electronics and NOR logic gates.³³ More generally, interfacing multiple nanowire inputs and outputs to neurons and neural networks enables one to stimulate, inhibit, or reversibly block signal propagation along specific pathways while simultaneously mapping signal flow throughout the network. This novel approach could be used to investigate synaptic processing in neural networks as well as to explore hybrid circuits for information processing and interfacing with neural prosthetics.

Conclusions

In this review, we have illustrated how nanowire-based field-effect sensor device arrays modified with specific surface receptors and/or interfaced to living cells represent a powerful and unique nanotechnology-enabled detection and interface platform for medicine and the life sciences, broadly defined. These nanowire

devices have a number of key features—including direct, label-free, and real-time electrical signal transduction; ultrahigh sensitivity; exquisite selectivity; and potential for integration of addressable arrays on a massive scale—that set them apart from all other sensor technologies available today. The examples described in this review illustrate unique capabilities for multiplexed real-time detection of proteins and single viruses that have immediate and significant consequences for healthcare and bioterrorism. Moreover, the direct electrical recording, stimulation, and inhibition of single neurons opens up new and exciting opportunities for neuroscience, cell diagnostics, and novel strategies for hybrid information processing.

Acknowledgments

We graciously thank the scientists cited in this review for their contributions to the research. Charles M. Lieber acknowledges generous support from the Defense Advanced Research Projects Agency, the

National Cancer Institute, Applied Biosystems, and the Ellison Medical Foundation.

References

1. J.T. Hu, T.W. Odom, and C.M. Lieber, *Acc. Chem. Res.* **32** (1999) p. 435.
2. C.M. Lieber, *MRS Bull.* **28** (July 2003) p. 486.
3. Y. Li, F. Qian, J. Xiang, and C.M. Lieber, *Mater. Today* **9** (10) (2006) p. 18.
4. Z.L. Wang, *Mater. Today* **7** (6) (2004) p. 26.
5. L. Samuelson, *Mater. Today* **6** (10) (2003) p. 22.
6. P. Yang, *MRS Bull.* **30** (February 2005) p. 85.
7. F. Patolsky and C.M. Lieber, *Mater. Today* **8** (4) (2005) p. 20.
8. F. Patolsky, G. Zheng, and C.M. Lieber, *Anal. Chem.* **78** (2006) p. 4261.
9. F. Patolsky, G. Zheng, and C.M. Lieber, *Nanomedicine* **1** (2006) p. 51.
10. A. Morales and C.M. Lieber, *Science* **279** (1998) p. 208.
11. Y. Cui, Q. Wei, H. Park, and C.M. Lieber, *Science* **293** (2001) p. 1289.
12. J. Hahn and C.M. Lieber, *Nano Lett.* **4** (2004) p. 51.
13. W.U. Wang, C. Chen, K.H. Lin, Y. Fang, and C.M. Lieber, *Proc. Natl. Acad. Sci. USA* **102** (2005) p. 3208.

14. F. Patolsky, G.F. Zheng, O. Hayden, M. Lakadamyali, X.W. Zhuang, and C.M. Lieber, *Proc. Natl. Acad. Sci. USA* **101** (2004) p. 14017.
15. G. Zheng, F. Patolsky, Y. Cui, W.U. Wang, and C.M. Lieber, *Nat. Biotechnol.* **23** (2005) p. 1294.
16. Y. Cui and C.M. Lieber, *Science* **291** (2001) p. 851.
17. Y. Cui, Z.H. Zhong, D.L. Wang, W.U. Wang, and C.M. Lieber, *Nano Lett.* **3** (2003) p. 149.
18. G. Zheng, W. Lu, S. Jin, and C.M. Lieber, *Adv. Mater.* **16** (2004) p. 1890.
19. J. Xiang, W. Lu, Y. Hu, Y. Wu, H. Yan, and C.M. Lieber, *Nature* **441** (2006) p. 489.
20. S.M. Sze, *Physics of Semiconductor Devices* (Wiley, New York, 1981).
21. Y. Huang, X.F. Duan, Q.Q. Wei, and C.M. Lieber, *Science* **291** (2001) p. 630.
22. R. Etzioni, N. Urban, S. Ramsey, M. McIntosh, S. Schwartz, B. Reid, and J. Radich, *Nat. Rev. Cancer* **3** (2003) p. 1.
23. J.D. Wulfschuh, L.A. Liotta, and E.F. Petricoin, *Nat. Rev. Cancer* **3** (2003) p. 267.
24. U. Windhorst and H. Johansson, *Modern Techniques in Neuroscience Research: Electrical Activity of Individual Neurons In Situ: Extra- and Intracellular* (Springer, New York, 1999).
25. P. Fromherz, *ChemPhysChem* **3** (2002) p. 276.
26. A.D. Oviedo and J. Reyes, *J. Neurosci.* **25** (2005) p. 4985.
27. A. Lambacher, M. Jenkner, M. Merz, B. Eversmann, R.A. Kaul, F. Hofmann, R. Thewes and P. Fromherz, *Appl. Phys. A* **79** (2004) p. 1607.
28. A. Offenhausser, C. Sprossler, M. Matsuzawa, and W. Knoll, *Biosens. Bioelectron.* **12** (1997) p. 819.
29. M. Merz and P. Fromherz, *Adv. Funct. Mater.* **15** (2005) p. 739.
30. M. Voelker and P. Fromherz, *Small* **1** (2005) p. 206.
31. C.D. James, A.J.H. Spence, N.M. Dowell-Mesfin, R.J. Hussain, K.L. Smith, and H.G. Craighead, *IEEE Trans. Biomed. Eng.* **51** (2004) p. 1640.
32. Y. Jimbo, N. Kasai, K. Torimitsu, T. Tateno, and H.P.C. Robinson, *IEEE Trans. Biomed. Eng.* **50** (2003) p. 241.
33. F. Patolsky, B.P. Timko, G. Yu, Y. Fang, A.B. Greytak, G. Zheng, and C.M. Lieber, *Science* **313** (2006) p. 1100.
34. S. Jin, D. Whang, M.C. McAlpine, R.S. Friedman, Y. Wu, and C.M. Lieber, *Nano Lett.* **4** (2004) p. 915.
35. A.T. Gullledge and G.J. Stuart, *J. Neurosci.* **23** (2003) p. 11363.
36. M.E. Larkum and J.J. Zhu, *J. Neurosci.* **15** (2002) p. 6991.
37. L.R. Squire, J.L. Roberts, N.C. Spitzer, and M.J. Zigmond, *Fundamental Neuroscience* (Elsevier Science, San Diego, 2003). □

Missing Important Issues of MRS Bulletin?

Back Issues are still available! Contact MRS for details—



506 Keystone Drive, Warrendale, PA 15086-7573 U.S.A.

Tel: 724-779-3003 • Fax: 724-779-8313

E-mail: info@mrs.org • www.mrs.org/bulletin



Trace Elemental Analysis, Worldwide

World Leaders in Glow Discharge Mass Spectrometry

- Trace and Ultra Trace Elemental Analysis Laboratory
- Bulk, Near Surface and Depth Profile Elemental Evaluation
- Conductive, Non Conductive and Semi Conductive Materials Analysis from H to U (solids and powders)
- Minimum sample requirements (less than one gram required for 75 elements scan)
- Analytical Capabilities
 - Trace Elemental Analysis by GD/MS
 - Compositional Analysis by ICP-OES
 - Metallography
 - C and S by Combustion Technique
 - N,O, H by Inert Gas Fusion

ISO 9002, NADCAP, GE—S400

Lab facilities in US, Europe and Asia



Shiva Technologies Inc.

6707 Brooklawn Parkway
Syracuse, NY 13211
Phone: 315-431-9900
Fax: 315-431-9800
sales@shivathec.com

www.shivathec.com